Global J. Environ. Sci. Manage. 10(3): 1067-1084, Summer 2024, Serial #39

Global Journal of Environmental Science and Management
(GJESM)

Homepage: https://www.gjesm.net/

Podcasts

ORIGINAL RESEARCH PAPER

Removal of direct navy blue dye from aqueous solutions using banana peels

F. Fuentes-Gandara[1], I. Piñeres-Ariza[2], A. Zambrano-Arevalo[3], G. Castellar-Ortega[4], C. Herrera-Herrera[1], S. Castro-Muñoz[5], G. Peluffo-Foliaco[5], J. Pinedo-Hernández[6]

[1] *Department of Natural and Exact Sciences, Universidad de la Costa, Calle 58, Barranquilla, Colombia*

[2] *Department of Physics, Faculty of Basic Sciences, Universidad del Atlántico, Antigua vía Puerto Colombia, Colombia*

[3] *Faculty of Health Sciences, Universidad Libre, Cra 51B #135 -100, Barranquilla, Colombia*

[4] *Faculty of Engineering, Universidad Autónoma del Caribe, Calle 90 # 46-112, Barranquilla, Colombia*

[5] *Department of Civil and Environmental, Universidad de la Costa, Calle 58, Barranquilla, Colombia*

[6] *Faculty of Basic Sciences, Department of Chemistry, Universidad de Córdoba, Cra 6 #77-305, Montería, Colombia*

ARTICLE INFO

Article History:
Received 27 December 2023
Revised 01 March 2024
Accepted 05 April 2024

Keywords:
Adsorption
Banana peel
Biochar
Isotherms
Navy blue dye
Textile industry

DOI: 10.22034/gjesm.2024.03.09

ABSTRACT

BACKGROUND AND OBJECTIVES: The textile industry is known to produce large amounts of dyes and other harmful contaminants. This issue is of great importance as it adversely affects both water resources and the well-being of organisms. To address this issue, biochar is frequently used as a sustainable and environmentally friendly material for removing chemical contaminants during wastewater treatment. The aim of this study was to evaluate the viability of utilizing biochar obtained from banana peels as a promising bioadsorbent for reducing environmental pollution caused by direct navy blue dye. The research investigated various factors such as temperature, potential of hydrogen levels, particle size, and concentrations to determine the effectiveness of biochar in dye removal.

METHODS: The biochar obtained was separated into powdered and granular forms based on particle sizes of 425 and 850 micrometer, respectively. The biochar's textural characteristics were assessed through nitrogen adsorption/desorption isotherms. Fourier transform infrared spectroscopy and the Boehm method were employed to analyze and measure organic functional groups, specifically acidic groups, for identification and quantification purposes. Batch experiments were performed to ascertain the effects of the initial concentration and potential of hydrogen on the adsorption capacity and removal percentage.

FINDINGS: The results indicated that the powdered biochar obtained at 500 degrees Celsius had the higher surface area, with a value of 80.4 square meter per gram. The biochar demonstrated remarkable removal percentages, achieving 97 percent at the lowest concentration and 89 percent at the highest concentration, when the potential of hydrogen was adjusted to a value of 6. The Freundlich model gave the best fit to the experimental data for this biochar and obeyed pseudo second order kinetics, with correlation coefficients of 0.93 and 0.99, respectively.

CONCLUSION: This study provides evidence of the high removal efficiency achieved by biochar derived from banana peel waste in the removal of direct navy blue dye. Precise temperature control during the calcination process is essential to ensure its favorable chemical and textural properties. The unique attributes of banana peel biochar position it as an exceptionally promising adsorbent material. Not only is it cost-effective and environmentally friendly, but it also outperforms current wastewater treatment technologies in terms of competitiveness. Its remarkable ability to reduce contaminants, particularly the removal of dyes, further solidifies its potential as a highly effective solution.

NUMBER OF REFERENCES 74

NUMBER OF FIGURES 6

NUMBER OF TABLES 5

*Corresponding Author:
Email: *fabioar20@hotmail.com*
Phone: +300 5616 226
ORCID: 0000-0002-0681-0544

Note: Discussion period for this manuscript open until October 1, 2024 on GJESM website at the "Show Article".

INTRODUCTION

Water pollution caused by industrial wastewater is a significant global issue that demands immediate attention. The contamination of water resources has emerged as one of the most critical problems faced by societies worldwide. Due to its complicated structure, low biodegradability, and high toxicity, wastewater has the potential to negatively impact ecosystems. Various industries, such as textiles and agrochemicals, produce pesticides, dyes and other potentially toxic chemical products, which are subsequently discharged into water bodies, representing a serious threat to the quality of water resources, biota, and even human health (Guo *et al.,* 2023). The increasing demand for synthetic dyes within the textile and clothing industry has caused a significant upsurge in the volume of wastewater that contains these dyes (Katheresan *et al.,* 2018). There are various technologies used in the removal of these substances, including ozonation, advanced oxidation processes, nanofiltration, ultrafiltration, chemical precipitation, chemical coagulation/flocculation, ion exchange and reverse osmosis (Wang *et al.,* 2022). Many of these technologies are not viable because of their expensive operational expenses (Samimi, 2024) and the generation of byproducts (Castellar Ortega *et al.,* 2020) and are sometimes difficult to apply on a large scale in the treatment of industrial wastewater. Adsorption technology has become increasingly important in recent years as a viable solution for eliminating synthetic dyes (Castellar Ortega *et al.,* 2022). This method offers several advantages, including its simplicity of use, affordability, minimal secondary environmental impact, and remarkable effectiveness in capturing pollutants (Hu *et al.,* 2022; Wang *et al.,* 2018). Importantly, these benefits align perfectly with the 12 principles of green chemistry established by the Environmental Protection Agency (EPA, 2024). Biochar-derived adsorbents have found extensive application in the field of environmental remediation owing to their renewable nature, economical viability, customizable porosity, and abundant functional groups (Han *et al.,* 2018; Zhao *et al.,* 2021). Biochar can be obtained from various raw materials, including plant-based, agricultural, and fruit and vegetable residues (Ding et al., 2023). Different thermochemical processes, such as torrefaction, carbonization and pyrolysis, are used for biochar production (Patra *et al.,* 2021). Pyrolysis stands out as the most straightforward, budget-friendly, and exceptionally productive technique (Kumar *et al.,* 2020). Several studies have reported biochar production with the biomass from fruit seeds, leaf litter, banana residues, melon peels and coconut shells (El Nemr *et al.,* 2021; Mukherjee *et al.,* 2021). The effluents discharged by the textiles, leather, paper, and pulp industries primarily consist of dyes or colorants (Deka *et al.,* 2022). These substances have serious toxic effects on the environment and human health (Ewuzie *et al.,* 2022). Researchers have highlighted the effectiveness of biochar obtained from fruit waste in adsorbing intricate dyes. Wu *et al.* (2020) used biochar obtained from litchi peels to remove congo red and malachite green dyes from wastewater and achieved removal efficiencies of 2468 and 404.4 milligrams per gram (mg/g), respectively. The biochar derived from litchi peel demonstrated strong reproducibility while avoiding any additional environmental concerns. Biochar prepared from pineapple fruit peel was evaluated for the removal of patent blue dye and showed a maximum removal rate of 95 percent (%) at potential of hydrogen (pH) 2 (Kapoor *et al.,* 2022). Biochar derived from avocado peels effectively eliminated methylene blue from wastewater, demonstrating exceptional durability and the ability to be reused for up to four cycles of sorption and desorption. The material exhibited an impressive adsorption capacity of 62.1 mg/g (Prabakaran *et al.,* 2022). Bananas are among the most consumed fruits and are primarily grown in tropical countries (Drenth and Kema, 2021). Bananas are the second most produced fruit worldwide, making up around 16% of total fruit production. They rank as the fourth most significant food crop, following rice, wheat, and maize (Alzate Acevedo *et al.,* 2021). After harvest, approximately 60% of the banana biomass is wasted. Internationally, approximately 114.1 million metric tons of banana waste are generated, which leads to environmental problems such as excessive greenhouse gas emissions. The banana industry produces unused biomass waste such as pseudostems, leaves, rachises, and fruit peels. It is estimated that the fruit constitutes only 12% of the total mass of the banana (Ahmed *et al.,* 2019). Peels constitute 35–50% of the total weight of the fruit, an untapped biomass commonly discarded as waste (Singh *et al.,* 2018). Colombia ranks eleventh globally as a banana producer and ranks fifth in Latin

America, following Brazil, Ecuador, Guatemala, and Costa Rica, Food and Agriculture Organization of the United Nations Statistical Database (FAOSTAT, 2022). Banana production in Colombia ranges across the entire country. In 2020, the country generated approximately 2.4 million tons of bananas (FAOSTAT, 2022). Both small and large producers participate in the production process, dividing their output between exports and the local market. On average, there are 35139 agricultural production units dedicated to this activity in the country, Ministerio de Agricultura y Desarrollo Rural (MADR, 2020). The residues consist of significant industrial components, including natural fibers, cellulose, and hemicellulose. These components can be altered through various methods, such as bacterial fermentation and anaerobic degradation, to produce a wide range of products, from bioplastics to biofuels. This contributes to the advancement of a circular economy. They can also be used in wastewater treatment through the development of low-cost biofilters and the production of carbon from banana rachises and peels (Alzate Acevedo *et al.,* 2021). The waste derived from banana cultivation has been investigated for the removal of various pollutants, such as heavy metals (Lapo *et al.,* 2020; Baldovi *et al.,* 2022; Das *et al.,* 2022), as well as for the degradation of various dyes, including congo red (Mondal and Kar, 2018), emerald green (Rehman *et al.,* 2019), evans blue (Basirun *et al.,* 2023), setapers blue (Bourechech *et al.,* 2023), and direct blue 86 (Barboza *et al.,* 2024). Nevertheless, limited research has been conducted on the elimination of direct navy blue dye (DNB) by utilizing agro-industrial residues. Among these, the work of Miranda-Mandujano *et al.* (2018) employing industrial soybean residues stands out, as well as the study by Castellar *et al.* (2020), which was focused on coffee grounds. Orange peels have proven to be a cost-efficient bioabsorbent for effectively eliminating DNB dye from textile effluents (Khaled *et al.*, 2009; Irem *et al.* 2013). The biomass of silk tree leaves has also been used as a natural adsorbent for the removal of this dye, commonly employed in fabric dyeing (Jayanthi and Sudarmanigayathri, 2015). The byproduct obtained during the creation of bio-hydrogen using the water hyacinth plant has shown to be a highly effective and economical adsorbent for eliminating DNB dye from wastewater in the textile industry (Kanchi *et al.,* 2017). Despite the reported studies on the application of bioadsorbents derived from agro-industrial wastes, there remains a significant research gap concerning the potential utilization of banana peels for DNB dye removal in wastewater from the textile industry. Within this framework, utilizing banana peels to create bioadsorbents presents a hopeful remedy. This method not only aids the agro-industrial field in repurposing waste but also plays a constructive role in environmental preservation by halting the decay of these peels, lessening greenhouse gas emissions, addressing climate change, and minimizing chemical pollutants in the textile industry. Given the significant banana production in Colombia and the waste generated by domestic consumption throughout the year, banana peels are a valuable source of biomass with enormous valorization potential. This byproduct is an extremely stable biochar that has the potential to serve as an environmentally friendly and affordable absorbent for the removal of dyes. The objective of this study is to evaluate the effectiveness of different biochars derived from fully ripened banana peels in removing DNB dye from aqueous solutions. The batch adsorption technique will be employed, with variations in temperature, particle size, pH, and initial concentration of the solutions being investigated. Models were developed to match the adsorption equilibria and kinetic data. The current study was conducted at the Chemistry Laboratory, Department of Natural and Exact Sciences, Universidad de la Costa and Universidad del Atlántico, Colombia in 2021.

MATERIALS AND METHODS

The methodology consists of two main components: the production of biochar from discarded banana peels, which are heated to temperatures of 300 and 500 degrees Celsius (°C), and subsequent characterization. The characterized adsorbent is tested using initial concentration studies, particle size, and pH with the batch adsorption technique to determine pollutant removal efficiency, specifically targeting DNB dye from aqueous solutions.

Biochar preparation

Ripe bananas were obtained from different stores in the market of Barranquilla city, Colombia. The phloem (edible part of the banana) was removed, and the banana peels were uniformly cut into small pieces. Some of these samples were heated at 300

°C for 2 hour (h), while the remaining portion was heated at 500 °C for 1 h in an air atmosphere. The samples were crushed and sieved to give particle sizes of 425 and 850 micrometers (µm). The material obtained was rinsed with ultrapure water until the liquid above it lost its color, then dried at 100 °C for 1 h. The obtained biochars were classified based on their particle sizes (powdered or granular) and processing temperature (300 or 500 °C).

Physicochemical characterization of biochar

The surface areas of the biochars were determined with the Brunauer, Emmett, and Teller (BET) method employing a Micromeritics Gemini III 2375 sorptometer (Benkő *et al.,* 2013). The specific surface area of the biochar was determined through nitrogen adsorption/desorption isotherms during the process. This technique is crucial for evaluating the biochar's adsorption capacity and porous structure. The standard tests for volatile matter, moisture, and ash content of the biochar derived from banana peels were performed according to American Society for Testing Materials (ASTM) ASTM D 5832, ASTM D 2867, and ASTM D 2866, respectively (Pereira *et al.,* 2018). Functional groups in the biochar were partially quantified through the application of the Boehm method during chemical characterization. To quantify the organic functional groups, 0.5 gram (g) of each biochar was added to 50 milliliter (mL) of 0.1 molarity (M) solutions of sodium hydroxide (NaOH), sodium carbonate (Na_2CO_3), sodium bicarbonate ($NaHCO_3$), and hydrochloric acid (HCl) for 24 h each. A sample was collected and analyzed by titration, utilizing standard solutions of NaOH and HCl as required. All analytical grade chemical reagents utilized were obtained from Merck. The number of acid sites on the biochar was calculated by assuming that NaOH neutralized carboxylic, lactonic, and phenolic groups; Na_2CO_3 neutralized carboxylic and lactonic groups; and $NaHCO_3$ neutralized carboxylic groups (Fidel *et al.,* 2013). The number of active acidic sites was expressed as milliequivalent per gram (mEq/g) of dry sample and was determined using Eq. 1 (Hernández *et al.,* 2019):

$$\left[{}^{mEq}/_{g}\ neutralized \right] = \frac{\left(C_i - C_f \right) \times V}{m_{CA}} \times 100 \quad (1)$$

Where; C_i and C_f = initial and final concentrations, respectively, of the solution.

V= volume of solution used in liter (L).

m_{CA} = mass of activated carbon in grams.

The identification of functional groups, particularly organic acids, was conducted via Fourier transform infrared spectroscopy (FTIR) utilizing Shimadzu instrumentation. Spectra were collected using a resolution of 2/centimeter (cm) and a scanning velocity of 20 scans/minute. The frequency range was 4000 to 400/cm (Ahmad *et al.,* 2007).

Batch study

Preparation of a standard solution involved adding 0.010 g of DNB to 100 mL of distilled water, resulting in the acquisition of a calibration curve. Then, different solutions with concentrations between 0 and 10 milligram per liter (mg/L) were prepared by taking aliquots of 2, 4, 6, 8, and 10 mL and diluting them to 100 mL with distilled water in all cases. The absorbance of each solution was determined at 540 nanometers (nm), the wavelength of maximum absorption, after conducting a preliminary scan with a DR3900 Hach spectrophotometer. The concentration of the dye showed a direct correlation with the absorbance values. The task was executed three times in order to confirm reproducibility. A 500 mg/L stock solution of DNB was prepared by dissolving the required amount of DNB in distilled water. From this solution, concentrations of 10, 60, 120, 300, 400, and 500 mg/L were prepared, and the pH was adjusted to 6, 9, and 12 with diluted HCl and NaOH. For the adsorption tests, 20 mL of each DNB dye dilution was taken, and 0.2 g of biochar was added. The samples were positioned on a flat shaker, rotating at a speed of 120 revolutions per minute (rpm) for a duration of 8 h at a temperature of 23 °C (Ahmad *et al.,* 2007). The filtration process was applied to the samples, followed by measuring the concentration of the resulting solution at a wavelength of 540 nm using a DR3900 HACH spectrophotometer. Three replicates were conducted for each experiment, covering the four types of charcoals (granular at 300 °C and 500 °C, powdered at 300 °C and 500 °C), resulting in a total of 216 processed samples, allowing obtained the best conditions of operation depending on pH, type of biochar, temperature and concentration, which contribute to the variability of the response (removal of DNB dye) in aqueous solutions, considering the

hypothesis that calcined banana peels will effectively adsorb the DNB dye from aqueous solutions due to their porous structure, carboxylic acids, and phenols. Factors like temperature and pH are expected to influence adsorption efficacy.

For the kinetic study, 0.2 g samples of biochar were placed in 20 mL of DNB dye solution with a concentration of 120 milligram per milliliter (mg/mL) and shaken on a horizontal shaker. Each sample was filtered, and concentration measurements were taken every 60 minutes (/min) for 8 h (60, 120, 180, 240, 300, 360, 420, and 480/min) using an ultraviolet visible (UV–Vis) spectrophotometer.

Adsorption capacities

Based on the findings derived from the equilibrium experiments, the percentage of DNB removal was calculated for each of the analyzed systems utilizing Eq. 2 (Kumar *et al*., 2023):

$$[\%R] = \frac{(C_O - C_e)}{C_O} \times 100 \quad (2)$$

Where, C_0 (mg/L) is the initial concentration of DNB and C_e (mg/L) is the equilibrium concentration. The equilibrium adsorption capacity of the biochar q_e (mg/g) was calculated using Eq. 3 (Kumar *et al*., 2023).

$$[q_e] = \frac{(C_o - C_e) \times V}{W} \quad (3)$$

Where, W(g) is the adsorbent mass.

RESULTS AND DISCUSSION

Physicochemical characterization of biochar

Table 1 shows the surface areas, external areas, and microporosities of the samples. Calcination of the granular and powdered biochar at 500 °C led to the development of micro- and mesopores in the material. This phenomenon may be associated with the oxidation process of the organic material (Priya *et al.,* 2023) present in the banana peel when heated at 500 °C. During this thermal process, the material's surface area significantly increased compared to the original material, resulting in the creation of substantial porosity. The findings aligned with the study by Pan *et al.* (2021), which indicated that elevated temperatures hastened the development of pores in the biochar, leading to an augmentation in the specific surface area. Table 1 shows the powdered biochar had particles measuring 450 nm, and the average particle size of the granular biochar was 850 nm.

Table 2 displays the moisture, volatile matter, and ash content percentages for the four biochar samples. These results revealed that the moisture percentage did not significantly depend on the calcination temperature. The volatile material exhibited a strong correlation with the calcination temperature, highlighting a significant impact. At 500 °C, the percentages of volatile material in both the powdered and granular biochars were higher than those generated at 300 °C. The trend observed during this thermal treatment led to a more pronounced breakdown of low molecular weight components like hemicellulose, lignin, and cellulose (Mishra *et al.,* 2023). The ash content results revealed that the granular biochar produced at a temperature of 300 °C displayed a higher amount of noncombustible residue. This behavior was consistent with the results reported by Sinha *et al.* (2019). Using thermogravimetric measurements, they reported that in the initial degradation stage at approximately 137.3 °C, hemicellulose, lignin, and cellulose were partially decomposed. Following this, a subsequent phase of decomposition occurred within the temperature range of 137.3 to 448 °C, revealing once again the breakdown of hemicellulose and cellulose. Consequently, the biochar subjected to 300 °C did not experience complete degradation, resulting in a higher ash content in comparison.

The quantification of functional groups in the biochars was carried out through titrations. In order to determine the specific groups, either basic or acidic

Table 1: Textural properties of the biochar samples

Biochars	Surface area	External area	Micropore area
Powdered 300 °C	10.97	0.77	10.2
Granular 300 °C	15.95	0.55	15.4
Powdered 500 °C	80.4	30.4	50.0
Granular 500 °C	74.0	32.0	43.0

Values were expressed in square meter per gram (m^2/g)

Table 2: Percentages of moisture, volatile matter, and ash content in the different biochar samples

Biochars	Moisture (%)	Volatile matter (%)	Ash (%)
Powdered 300 °C	8.47	8.63	14.70
Granular 300 °C	8.04	1.29	23.80
Powdered 500 °C	6.37	12.7	17.32
Granular 500 °C	8.04	41.0	13.50

Table 3: Quantification of surface organic functional groups in the biochars.

Biochars	Total acidity	Carboxylic acids	Lactones	Phenols
Powdered 300 °C	3.9	1.9	0.0	2.0
Granular 300 °C	3.7	1.8	0.0	1.9
Powdered 500 °C	2.9	0.0	1.1	1.8
Granular 500 °C	3.7	1.5	0.0	2.2

Values were expressed in mEq/g

compounds were commonly utilized. For instance, NaOH (acid dissociation constant pKa=15.74) was used to determine carboxylic, phenolic (with a pKa between 8-11), and lactone groups. Na_2CO_3 (pKa=10.25) was employed for carboxylic and phenolic acids, while $NaHCO_3$ (pKa=6.37) was used to neutralize carboxylic acids or phenolic groups. HCl was utilized to determine the quantity of hydroxyl (OH) groups. Table 3 presents the various organic acid functional groups and their quantities.

The analyzed biochars exhibited a high degree of similarity in their acidic sites, although slightly fewer were detected in the 500 °C biochar powder. Most of the biochars predominantly exhibited carboxylic and phenolic acid groups, suggesting that they are predominantly acidic adsorbents. The presence of higher amounts of acid groups signifies the existence of a greater number of oxygenated functional groups, thereby improving the efficiency of adsorption (Bello *et al.,* 2017; Bankole *et al.,* 2022). Fig. 1 presents the FTIR spectra for the biochars used in this study. A band associated with oxygen (O) – hydrogen (H) vibrations appeared between 3300 and 3600 /cm. The detection of carboxylic acids and phenols was validated, as detailed by scholars such as Prahas (2008), who quantified these elements utilizing the Böehm method. Bands corresponding to the stretching vibrations of carbon (C) C-H bonds appeared at 2900 to 2800/cm and provided evidence for organic matter in the alkane biochar that had been calcined at 300 °C (Pavia *et al.,* 2014). As the temperature of calcination increased to 500 °C, a gradual reduction in the intensities of these bands was observed across all samples. Bands between 2400 and 2300 /cm for all samples suggested the presence of carbon dioxide (CO_2) (Trachenko and Niedzielski, 2022), which was likely adsorbed from the atmosphere.

Batch study

Effects of the initial DNB dye concentration, pH, temperature, and particle sizes on biosorption

Figs. 2 and 3 show that the dye removal percentages decreased as the initial concentration increased for each of the adsorption conditions. However, the adsorption capacities increased independently of pH (Fig. 4). This was associated with the concentration gradient of the DNB in the adsorbent. With higher initial concentrations of DNB, there was a faster transport process, leading to an increase in biochar adsorption capacity. Throughout batch analyses, the solution volume was kept constant, resulting in lower dye presence at low concentrations compared to high concentrations. The retention of a steady absorbent mass led to the removal of a significant portion of the dye. However, some free spaces for adsorption might have remained and gradually became occupied as the concentration increased. The findings of this study demonstrated clear linear relationships between the adsorption capacities and concentrations across all samples. Two factors could explain these correlations: first, increased surface areas due to higher DNB concentrations, as demonstrated by Zavvar and Seyedi (2010); it is worth considering that this might be connected to the fact that elevated initial concentration values bolstered the transportation process, ultimately amplifying the adsorption capacity of biochar. (Castellar Ortega *et al.,* 2017). Within adsorption processes, the pH assumes

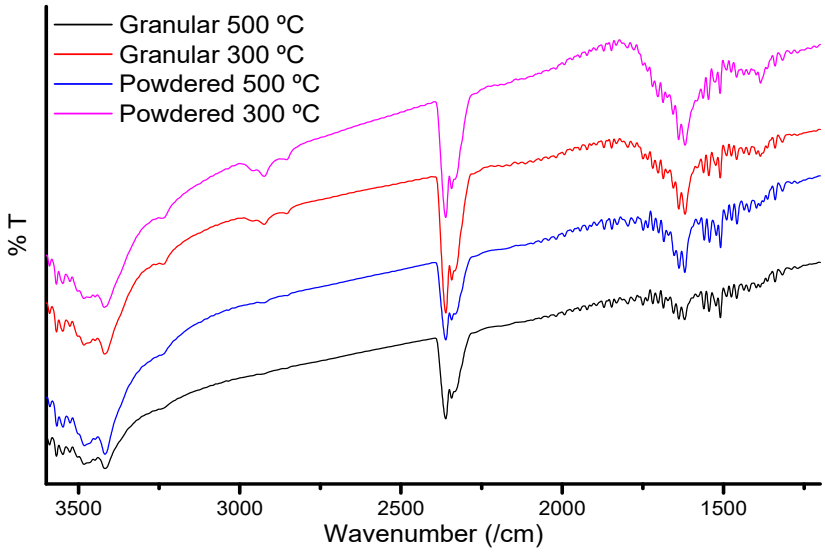

Fig. 1: FTIR spectra of the biochar samples. %T is percentage transmittance

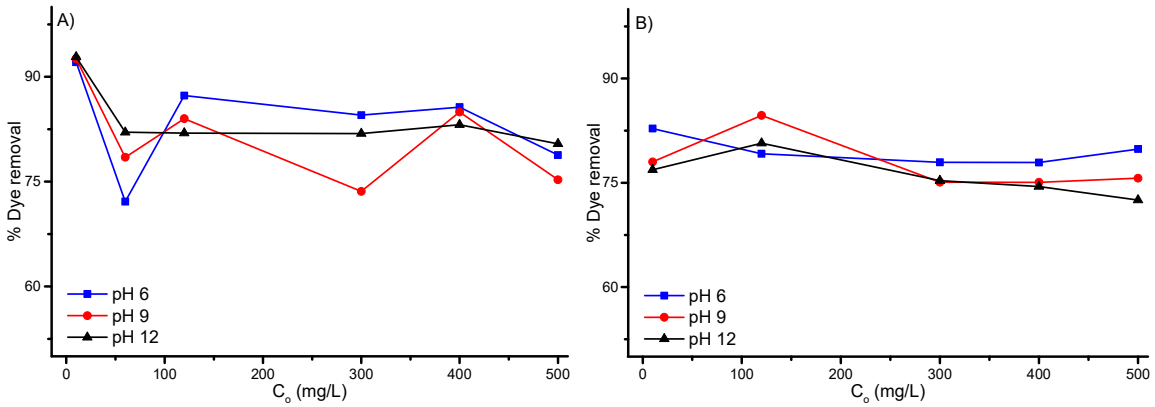

Fig. 2: Effect of the initial DNB concentration on the removal percentage for biochar prepared at 300 °C: A) Powdered and B) Granular

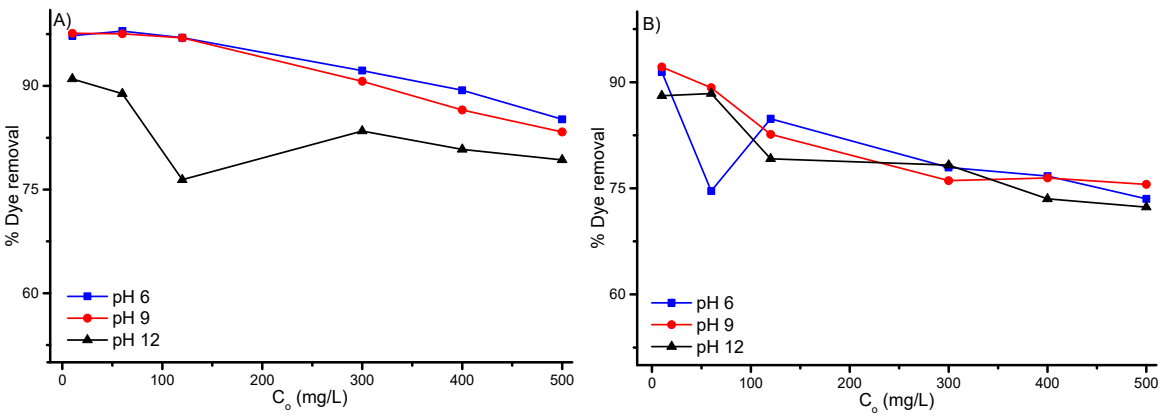

Fig. 3: Effect of the initial DNB concentration on the removal percentage for biochar prepared at 500 °C: A) Powdered and B) Granular

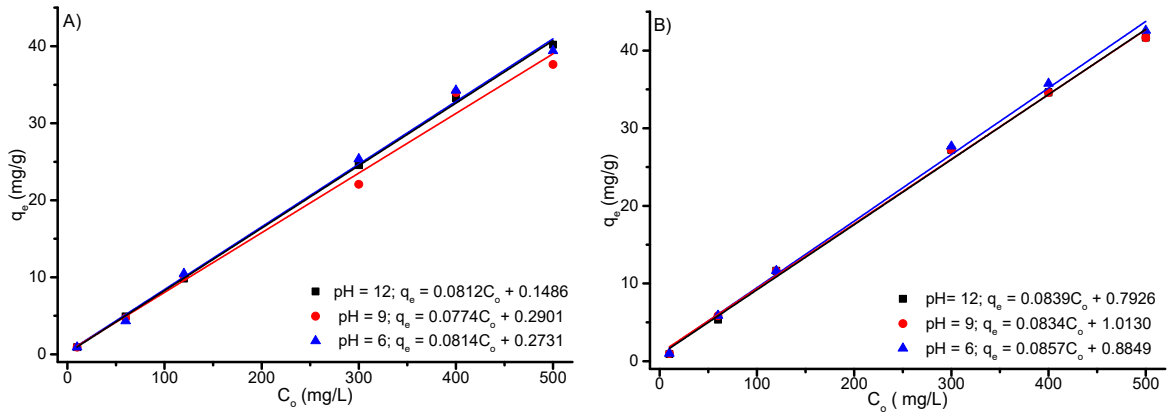

Fig. 4: Effect of the initial concentration on the adsorption capacities of biochars: A) Powdered 300 °C and B) Powdered 500 °C.

a critical role as it exerts a profound influence on the interactions taking place between the surface functional groups of both the adsorbent and adsorbate. The effectiveness of adsorption in acidic or basic solutions is determined by the characteristics of both biochar and dyes (Kapoor *et al.,* 2022). In this study, as the pH increased, the removal percentage of the dye decreased (Figs. 2 and 3). It can be inferred from the results that the lactones within the biochar underwent acidic hydrolysis at a pH of 6, causing an increase in suspension acidity. Additionally, this phenomenon may have facilitated electrostatic interactions with the sulfonate groups present in the dye (Castellar Ortega *et al.,* 2017). Furthermore, the biochar's inclusion of carboxylic acids and phenols allowed for the formation of physical interactions, like hydrogen bonds, that ultimately increased adsorption effectiveness. Increases in the solution pH led to more negative active sites, which hindered dye adsorption due to electrostatic repulsion (Nazir *et al.,* 2020). The results of this study are similar to those reported by Akter *et al.* (2021), who reported removal percentages close to 93% for textile effluent dyes adsorbed with banana peels at a pH of 7. The highest DNB removal percentages were observed for the powdered biochars obtained at both operating temperatures, with the pH adjusted to 6. In the case of biochar prepared at 300 °C, as the concentration of DNB dye changed from 10 to 500 mg/L, the removal percentage decreased from 92% to 82%. In contrast, the biochar that underwent heating at 500 °C displayed slightly elevated removal percentages. At the lowest concentration, it achieved a removal rate of 97%, while at the highest concentration, it reached 89%. These findings highlight the impact of temperature on the adsorption capacity, as higher temperatures expedite the intraparticle diffusion of the adsorbate within the pores (Guo *et al.,* 2003). The importance of particle sizes in biosorbents is undeniable, as a reduction directly translates into increased in the surface area of the adsorbent. This holds immense importance as it is closely associated with a significantly enhanced adsorption capacity, as evidenced by Asgher and Bhatti (2012). Increased particle sizes increased the removal efficiency of the powdered biochar, which was attributed to the availability of more accessible functional groups to interact with the dye molecules (Irem *et al.,* 2013). These findings were consistent with previous research, specifically the study conducted by Rodríguez *et al.* (2009), thus providing further support for the observed trend.

Adsorption isotherms and kinetics

The phenomenon of adsorption involves the attachment of liquid or gas molecules to the solid adsorbent (Dunne and Manos, 2010). The process entails the attraction of the adsorbate to the solid structure via diverse mechanisms until equilibrium is reached between the adsorbate and adsorbent phases. In this study, the adsorption capacities of the biochars were determined with the Freundlich (Hu *et al.,* 2019; Castellar Ortega *et al.,* 2013) and Langmuir (Nazir *et al.,* 2020; Castellar Ortega *et al.,* 2013) adsorption models. The Freundlich model sets forth a semiempirical connection where adsorption happens on a heterogeneous surface and spans multiple surface layers of the adsorbent, indicating

the occurrence of multilayer adsorption (Nazir *et al.,* 2020). Moreover, this model posits that the adsorption capacity grows alongside the rise in adsorbate concentration. The model is expressed mathematically using Eq. 4 (Hu *et al*., 2017):

$$qe = kCe^{1/n} \quad (4)$$

Where;

k is a constant associated with the adsorption capacity of the adsorbent (mg/g (L/g)$^{-1/n}$)

n is a constant related to the affinity (adsorption intensity) between the adsorbent and the solute. The values of n are always greater than 1. For strong adsorption, n falls between 2 and 10.

1/n is the inverse of the Freundlich constant (*n*)

The parameters k and n can be determined by linearizing the previous equation using Eq. 5 (Castellar Ortega *et al.,* 2022):

$$\ln q_e = \ln k + \frac{1}{n} \ln C_e \quad (5)$$

Where; lnq_e represents the natural logarithm of the equilibrium adsorption capacity

ln*k* is the natural logarithm of the Freundlich constant

lnC_e denotes the natural logarithm of the equilibrium concentration of DNB

The Langmuir model, conversely, relies on the interaction between molecules and the surface of the adsorbent, predominantly through physical forces. The model is based on the assumptions that adsorption takes place at uniform active sites on the adsorbent's surface, with consistent adsorption energies. Furthermore, once a solute occupies a site, no further adsorption can occur at that specific location (Murphy *et al.,* 2023). The model is expressed

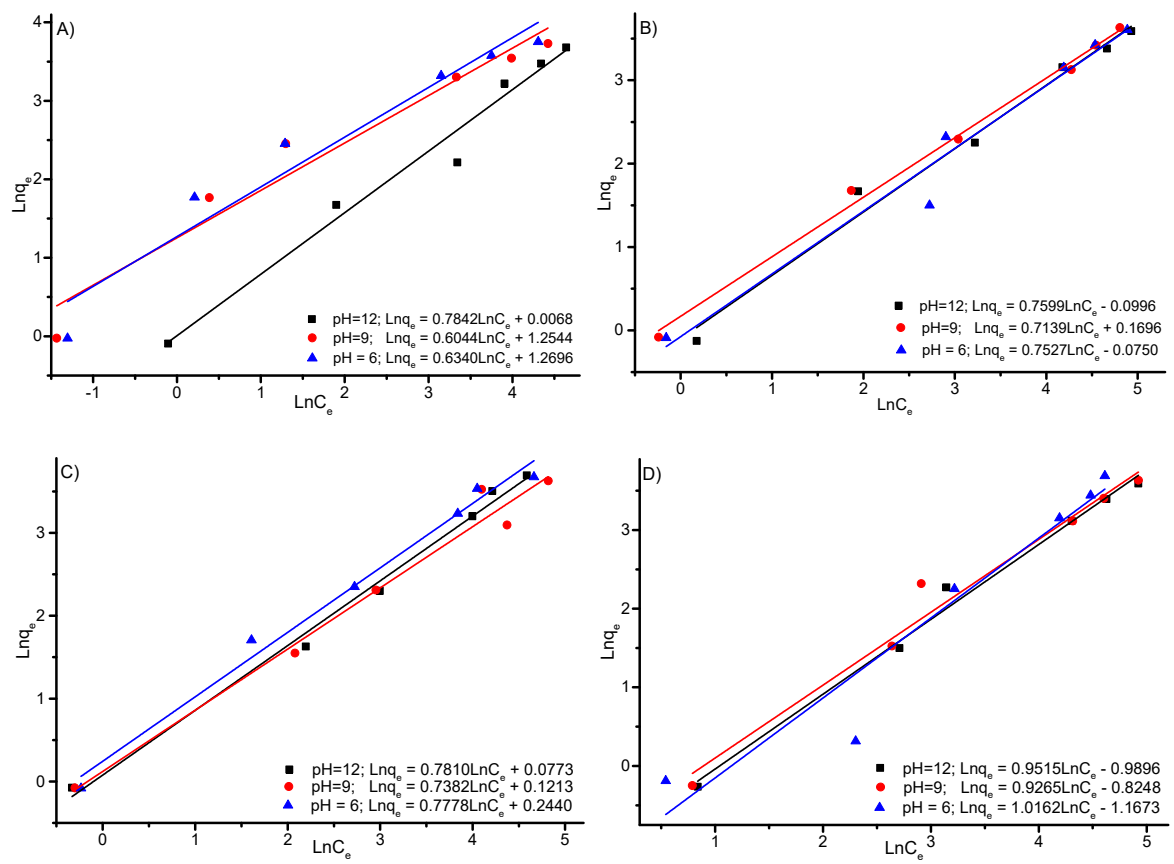

Fig. 5: Freundlich isotherms for the biochar samples: A) powdered 500 °C, B) granular 500 °C, C) powdered 300 °C and D) granular 300 °C

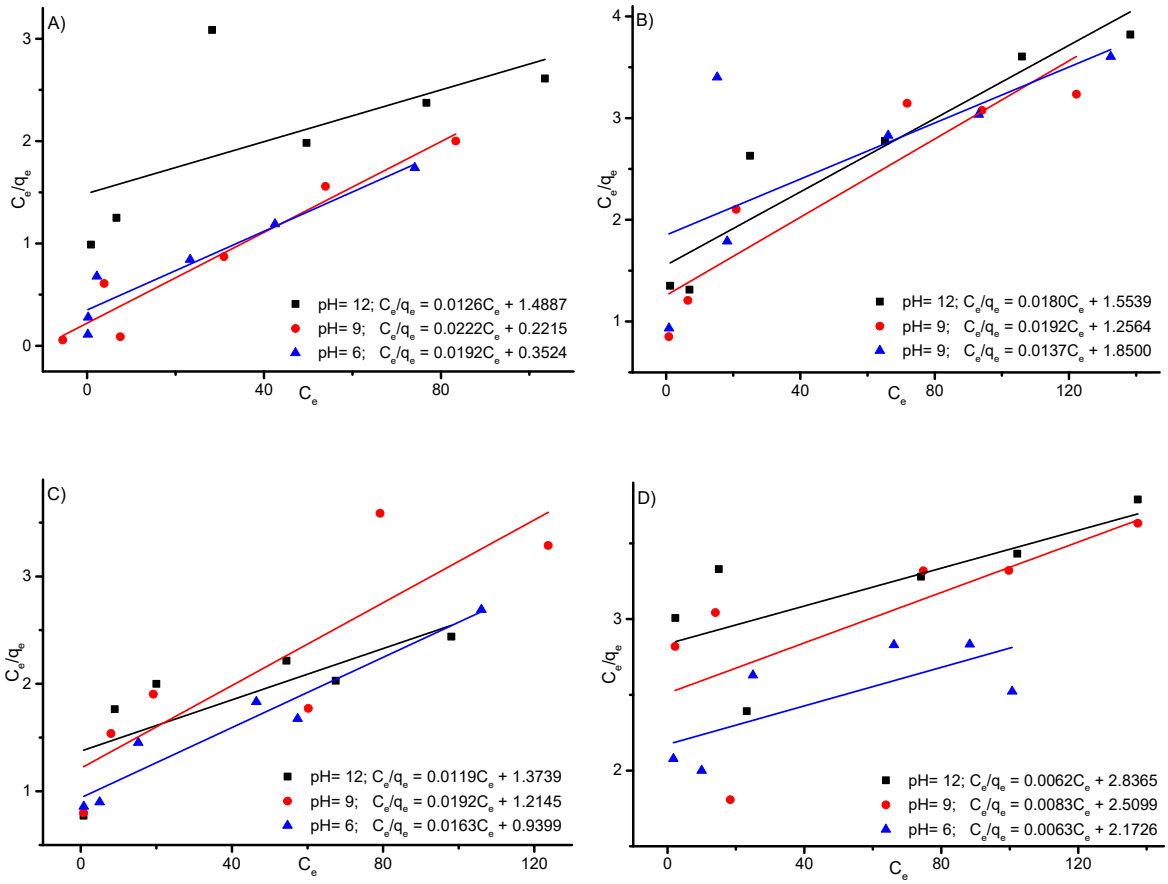

Fig. 6: Langmuir isotherms for the biochar samples: A) powdered 500 °C, B) granular 500 °C, C) powdered 300 °C and D) granular 300 °C

mathematically using Eq. 6 (Hu *et al.*, 2017):

$$qe = \frac{q_{max} B C_e}{1 + B C_e} \quad (6)$$

Where;

q_{max} = maximum amount of adsorbate that can be adsorbed per gram of adsorbent.

B = Langmuir constant indicating the affinity of the active sites.

It is possible to determine q_{max} and b by linearization of Eq. 7 (Castellar Ortega *et al.*, 2022):

$$\frac{C_e}{q_e} = \frac{C_e}{q_{max}} + \left(\frac{1}{B q_{max}} \right) \quad (7)$$

The main assumptions of the model are that adsorption occurs at identical active sites on the surf Figs. 5 and 6 show the fits of the experimental data with the Freundlich and Langmuir adsorption isotherm models. Table 4 summarizes the parameters of both models for both the powdered and granular biochar prepared at 300 and 500 °C. Based on the linear correlation coefficients, it was determined that the Freundlich model yielded better fits to the experimental data. The calculated values of n from fitting with the Freundlich model were mostly above unity, suggesting favorable adsorption with multilayer growth. However, upon examining the maximum adsorption capacities (q_{max} and k), it is observed that the Langmuir model exhibited higher DNB adsorption capacities for various biochars.

The following conditions were used to maximize the removal of DNB: powdered biochar prepared 500 °C, and a pH of 6. The initial dye concentration

Table 4: Kinetic and thermodynamic parameters for DNB adsorption

Biochars	pH	Langmuir constant, Correlación coefficient (R^2)	q_{max} (mg/g)	B (L/mg)	Freundlich constant, Correlation coefficient (R^2)	k (mg/g (L/mg)$^{-1/n}$)	n
	6	0.907	75.3	0.017	0.984	1.276	1.285
Powdered	9	0.676	51.8	0.015	0.972	1.28	1.354
300°C	12	0.506	74.0	0.086	0.991	1.08	1.280
	6	0.424	156.2	0.029	0.971	3.21	0.984
Granular 300	9	0.378	120.5	0.033	0.988	2.27	1.079
°C	12	0.392	151.3	0.021	0.988	2.69	1.050
	6	0.895	49.9	0.079	0.932	3.55	1.577
Powdered	9	0.915	45.4	0.080	0.941	3.50	1.654
500 °C	12	0.248	49.2	0.010	0.972	1.00	1.275
	6	0.348	72.5	0.074	0.963	0.92	1.328
Granular 500	9	0.818	52.1	0.015	0.994	1.18	1.400
°C	12	0.859	55.5	0.011	0.983	0.90	1.315
Kinetic models				Equation		Parameters	Statistics
Pseudo first order (PFO)				$ln(q_e - q_t) = lnq_e - k_1 t$		$q_{e,exp}$: 82.5 mg/g K_1: 0.77/h $q_{e,cal}$: 88.2 mg/g	R^2:0.97
Pseudo second order (PSO)				$\frac{t}{q_t} = \frac{1}{k_2 q_e^2} + \frac{t}{q_e}$		$q_{e,exp}$: 82.5 mg/g K_2:0.09/h $q_{e,cal}$: 88.07 mg/g	R^2:0.99

$\ln(q_e - q_t)$ represents the natural logarithm of the difference between the equilibrium adsorption capacity (q_e) and the adsorbate amount adsorbed at a specific time (q_t). $\ln q_e$ is the natural logarithm of the equilibrium adsorption capacity per unit mass of adsorbent. k_1 (/min) and k_2 (gram per milligram per minute g/mg·min) are the rate constants for pseudo-first-order and pseudo-second-order kinetics, respectively (Tovar-Gómez *et al.*, 2013; Largitte and Pasquier, 2016). *t* represents time, and qt is the amount adsorbed at time t.

was 60 mg/L, and aliquots were taken between 60 and 480 min. The PFO kinetic model, based on the Lagergren Equation 8, was applied. In this model, the effectiveness is determined by the solid's adsorption capacity, which designates an adsorption site on the adsorbent material for each chemical species found in the solution. This assumption plays a vital role in comprehending and simulating the adsorption kinetics, as described by Eq. 8 (Hu *et al*., 2017):

$$\ln\left(q_e - q_t\right) = \ln q_e - k_1 t \quad (8)$$

The PSO kinetic model was utilized, indicating that the adsorbate was absorbed by two active sites on the biomass and that the chemisorption process was the controlling factor. In this model, the rate at which adsorption occurs is determined by the surface chemistry and the interactions between the adsorbate and adsorbent, as expressed in Eq. 9 (Hu *et al*., 2017):

$$\frac{t}{q_t} = \frac{C_e}{k_2 q_e^2} + \frac{t}{q_e} \quad (9)$$

The DNB adsorption kinetics were evaluated with these models and the corresponding equations. The results are presented in Table 4, where the R^2 value for the PSO model was higher than that for the PFO model, indicating a better fit with the experimental data for the entire adsorption process. It can be inferred from this observation that the sorption process is primarily controlled by chemisorption, and the rate of adsorption is more influenced by the adsorption capacity rather than the concentration of DNB. Similar results were reported by Kanchi *et al.* (2017) and Khan *et al.* (2023).

Comparison with results from the literature

Table 5 presents a comparison of the obtained results with data reported in the literature for biochar prepared from organic solid waste. Despite the variations in processes and conditions, the results obtained were in line with previous reports on removal using alternative materials. t should be emphasized that while the biochar produced in this study exhibited less favorable surface characteristics than the materials discussed in previous research, it effectively removed DNB dye, proving its reliability.

Table 5: Comparison of the results obtained with those reported in the literature.

Biochar	AIM	Kinetic models	SA (m^2/g)	%R	Sources
BHFW-AC	Langmuir,Freundlich	Pseudo first order, pseudo second order	1242	94	Kanchi *et al.*, 2017
Orange peel	Langmuir,Freundlich	Pseudo first order, pseudo second order	-	82	Irem *et al.*, 2013
Orange peel	Langmuir,Freundlich	Pseudo first order, pseudo second order	-	92 - 97	Khaled *et al.*, 2009
Other conventional methods					
Electrochemical Oxidation	-	-	-	74.48	Ferreira *et al.*, 2023
UV irradiation (UV/Chlorine)	-	Pseudo first order	-	95.40	Detjob *et al.*, 2023
Magnetic geopolymer	Langmuir,Freundlich	Pseudo second order		86.29	Khan *et al.*, 2023
Electrocoagulation	-	-	-	85.00	Gohil and Makwana, 2019
coagulation–flocculation	Freundlich	Pseudo second order	-	41.50	Nourmoradi *et al.*, 2015
Banana peles	Langmuir,Freundlich	Pseudo first order, pseudo second order	80.4	89 - 97	The current study

BHFW-AC: Bio-hydrogen fermented waste, AIM: Adsorption isotherm models, SA: Surface area, %R: Percentage removal.

This was attributed to the adsorption capacities and cost-effectiveness, as reported by Kanchi *et al.* (2017), suggesting that despite differences in the processes and study conditions, the biochar from banana peels exhibited efficient removal of DNB from industrial textile effluents. Compared with other conventional DNB removal methods, such as electrochemical oxidation, UV/chlorine irradiation, magnetic geopolymer, electrocoagulation, and coagulation-flocculation, the banana peel absorption method shows comparable removal efficiency, reaching between 89 - 97%, even superior to methods such as coagulation-flocculation, electrochemical oxidation and electrocoagulation that do not exceed 85%. The significant level of efficiency already implies its benefit in terms of profitability by minimizing the requirement for further treatments or the adoption of multiple technologies to attain the equivalent level of removal DNB. Moreover, utilizing banana peels as absorbent material offers substantial economic benefits. In the food industry, banana peels are a commonly produced by-product that can be easily obtained in many regions at a low cost or even at no cost. The absorbent material is cost-effective compared to purchasing expensive chemicals or materials, making it a favorable option. However, limitations exist that may impact its effectiveness, such as selectivity for the contaminant, physicochemical properties of the wastewater, contact time, and biochar dosage.

CONCLUSION

The significant issue of pollution caused by dye waste is alarming because of its toxicity to different species. The release of these waste materials from the textile sector into the surrounding ecosystem gives rise to apprehensions from both a toxicological and aesthetic standpoint. This research showcased the efficacy of calcined banana peels in eliminating DNB from water-based solutions. Physicochemical characterization revealed the development of a porous structure after calcination, which, combined with the presence of carboxylic acids and phenols, may prove to be a useful adsorbent. The calcination temperature of biochar influences its volatile material content, being higher at 500 °C than at 300 °C, suggesting a more extensive decomposition of low molecular weight organic components at higher temperatures. The powdered biochar produced at 500°C demonstrated remarkable efficacy in removing DNB, achieving removal rates between 89% (500 mgDNB/L) and 97% (10 mgDNB/L) in solutions with a pH of 6. Enhancing the surface area of biochar particles is crucial as it allows for improved exposure of the adsorption active groups on the biochar surface. The isotherm models showed that the Freundlich model was most suitable for representing the adsorption

equilibria (R^2 > 0.93) with both the powdered and granular biochars at both operating temperatures. It can be inferred from this observation that the adsorption process took place on surfaces that were not uniform, resulting in the growth of multiple layers. When analyzing the experimental data using kinetic models, it was found that the pseudosecond-order equation provided an exceptional fit, as indicated by a linear correlation coefficient R^2 > 0.99. The results of this study indicate the potential of widely available banana peel waste as a raw material for adsorbents for the removal of synthetic dyes from water sources. This alternative has the potential to not just lower operating expenses, but also enhance process durations and efficiencies. To ensure the successful implementation of these contaminants and other operational variables on a pilot scale, it is imperative to conduct additional research that addresses the challenges they present.

AUTHOR CONTRIBUTIONS

F. Fuentes Gandara, the corresponding author, contributed to the data analysis and manuscript writing. I. Piñeres Ariza prepared most of the tables and figures and participated in manuscript preparation. A. Zambrano Arévalo supervised the experimental development and conducted a preliminary analysis of the data. G. Castellar Ortega contributed to the consolidation of the research proposal and critically reviewed the manuscript. C. Herrera Herrera supervised some of the experimental trials and interpreted their results. S. Castro Muñoz contributed to preparation and analysis of the samples. G. Peluffo Foliaco also participated in the preparation of the samples and in some laboratory experiments. J. Pinedo Hernández participated in the supervision, interpretation of the results, and manuscript preparation.

ACKNOWLEDGEMENT

The authors wish to extend their sincere gratitude to Universidad de la Costa and Universidad del Atlántico for providing the laboratories for the experimental development of this study.

CONFLICT OF INTEREST

The authors declare no potential conflict of interest regarding the publication of this work. In addition, the ethical issues including plagiarism, informed consent, misconduct, data fabrication and, or falsification, double publication and, or submission, and redundancy have been completely witnessed by the authors.

ABBREVIATIONS

$1/n$	Inverse of the Freundlich constant (n)
/cm	Per centimeter
/min	Per minute
µm	Micrometer
%	Percent
%R	Removal percentage
%T	Percentage transmittance
°C	Degrees Celsius
ASTM	American Society for Testing Materials
AIM	Adsorption isotherm models
ASTM	American Society of Testing and Materials
B	Langmuir constant indicating the affinity of the active sites

BET	Brunauer, Emmett and Teller
BHFW-AC	Bio-hydrogen fermented waste
C	Carbon
C_i	Initial concentration
C_0	Initial concentration
Ce	Concentration of adsorbate in the liquid phase at equilibrium
C_f	Final concentration
CO_2	Carbon dioxide
DNB	Direct navy blue dye
EPA	Environmental Protection Agency
Eq.	Equation
FAOSTAC	Food and Agriculture Organization of the United Nations Statistical Database
FTIR	Fourier Transform Infrared Spectroscopy
Fig.	Figure
h	Hour
H	Hydrogen
HCl	Hydrochloric acid
g	Gram
K	Constant associated with the adsorption capacity of the adsorbent
k_1	Rate constant for pseudo-first-order kinetics
k_2	Rate constant for the pseudosecond-order kinetic model
L	Liter
ln(k)	Natural logarithm of the Freundlich constant (*k*)
ln Ce	Natural logarithm of the concentration of adsorbate in the liquid phase at equilibrium
ln qe	Natural logarithm of the amount of adsorbate adsorbed at equilibrium per unit mass of adsorbent
ln(qe−qt)	Natural logarithm of the adsorbate amount not yet reached equilibrium (*qt*) at a specific time (*t*)
M	Molarity
MADR	Ministerio de Agricultura y Desarrollo Rural
mCA	Mass of biochar in grams
mEq/g	Milliequivalent per gram
mg/L	Milligram per liter
mg/mL	Milligram per milliliter
mg/g	Milligram per gram
m^2/g	Square meter per gram
$mg/g\ (L/g)^{1/n}$	Milligram per gram, multiplied by liter per gram raised to the inverse power of *n*
mL	Milliliter
n	Constant related to the affinity (adsorption intensity) between the adsorbent and the solute
nm	Nanometer
Na_2CO_3	Sodium carbonate
$NaHCO_3$	Sodium bicarbonate
NaOH	Sodium hydroxide
nm	Nanometer
O	Oxygen
OH	Hydroxyl
pH	Potential of hydrogen
pKa	Acid dissociation constant
PFO	Pseudo first order
PSO	Pseudo second order
qe	Equilibrium adsorption capacity
q_{max}	Maximum amount of adsorbate that can be adsorbed per gram of adsorbent
qt	Amount adsorbed at time t
R^2	Correlation coefficients for the Langmuir constant and Freundlich constant
rpm	Revolutions per minute
SA	Surface area
t	Time
UV–Vis	Ultraviolet visible
V	Volume of solution

W Adsorbent mass.

REFERENCES

Ahmad, A.; Loh, M.; Aziz, J., (2007). Preparation and characterization of activated carbon from oil palm wood and its evaluation on methylene blue adsorption. Dyes Pigment. 75(2): 263-272 (**10 pages**).

Ahmed, M.S.; Attia, T.; Abd El-Wahab, A.A.; Elgamsy, R.; Abd El-latif, M.H., (2019). Assessment of the physical properties of banana pseudo stem/ABS composites. IOP Conference Series: Mater. Sci. Eng., 634(1): 012023 (**9 pages**).

Alzate-Acevedo, S.; Díaz-Carrillo, J.; Flórez-López, E.; Grande-Tovar, D., (2021). Recovery of banana waste-loss from production and processing: a contribution to a circular economy. Molecules. 26(17): 5282 (**30 pages**).

Akter, M.; Rahman, F.; Abedin, M.; Kabir, S., (2021). Adsorption characteristics of banana peel in the removal of dyes from textile effluent. Textiles. 1: 361-375 (**15 pages**).

Asgher, M.; Bhatti, H.N., (2012). Evaluation of thermodynamics and effect of chemical treatments on sorption potential of citrus waste biomass for removal of anionic dyes from aqueous solutions. Ecol. Eng., 38(1): 79–85 (**7 pages**).

Baldovi, A.A.; Ayvazian, A.P.; Coelho, L.H.G.; de Jesus, T.A., (2022). Biosorption of Pb (II) by unmodified banana peel in batch and column experiments: a potential green and low-cost technology for industrial effluent treatment. Water Air Soil Pollut., 233: 490 (**10 pages**).

Bankole, D.; Oluyori, A.; Inyinbor, A., (2022). Potent adsorbent prepared from *Bilghia sapida* waste material: Surface chemistry and morphological characterization. Mater. Today Proc., 65: 3665-3670 (**6 pages**).

Barboza, J.A.T.; Penido, E.S.; Ferreira, G.M.D., (2024). Production of surfactant-modified banana peel biosorbents applied to treatment and decolorization of effluents. Colloid Surf. A-Physicochem. Eng. Asp., 680: 132650 (**15 pages**).

Basirun, A.A.; Othman, A.R.; Yasid, N.A.; Shukor, M.Y.A.; Khayat, M.E., (2023). A green approach of utilising banana peel (*Musa paradisiaca*) as adsorbent precursor for an anionic dye removal: kinetic, isotherm and thermodynamics analysis. Processes. 11(6): 1611 (**22 pages**).

Bello, O.; Owojuyigbe, S.; Babatunde, M.; Folaranmi, F., (2017). Sustainable conversion of agro-wastes into useful adsorbents. Appl Water Sci., 7(7): 3561-3571 (**11 pages**).

Benkő, M.; Puskás, S.; Király, Z., (2013). Application of mass spectrometry for study of the adsorption of multicomponent surfactant mixtures at the solid/solution interface. Adsorption. 19: 71-76 (**6 pages**).

Bourechech, Z.; Seghier, A.; Mokhtar, A., (2023). Assessment of physically treated banana leaves as a low-cost and eco-friendly adsorbent for removal of a textile azo dye. Biomass Convers. Biorefin., 13:14241-14252 (**12 pages**).

Castellar-Ortega, G.; Angulo, E.; Zambrano, A.; Charris, D., (2013). Adsorption equilibrium of methylene blue dye on activated carbon. Rev UDCA Act & Div Cient., 16(1): 263–271 (**9 pages**).

Castelar-Ortega, G.; Viloria, C.; Morrinson, B.; Angulo, M.; Zambrano, A., (2017). Evaluación de un carbón activado comercial en la remoción del colorante DB2. RECIA., 9(2): 164–170 (**7 pages**).

Castellar-Ortega, G.; Cely-Bautista, M.; Cardozo-Arrieta, B.; Angulo-Mercado, E.; Mendoza-Colina, E.; Zambrano-Arevalo, A.; Jaramillo-Colpas, J.; Rosales-Díaz, C., (2020). Removal of the direct navy-blue dye on modified coffee bean. Tecnología y Ciencias del Agua., 11(4): 1–26 (**26 pages**).

Castellar-Ortega, G.; Cely-Bautista, M.; Cardozo-Arrieta, B.; Jaramillo-Colpas, J.; Moreno- Aldana, L.; Valencia-Ríos, J., (2022). Evaluation of diatomaceous earth in the removal of crystal violet dye in solution. J. Appl. Res. Technol., 20(4): 387–398 (**12 pages**).

Das, J.; Saha, R.; Nath, H.; Mondal, A.; Nag, S., (2022). An eco-friendly removal of Cd (II) utilizing banana pseudo-fibre and *Moringa* bark as indigenous green adsorbent and modelling of adsorption by artificial neural network. Environ. Sci. Pollut. Res., 29(57): 86528-86549 (**22 pages**).

Deka, R.; Shreya, S.; Mourya, M.; Sirotiya, V.; Rai, A.; Khan, M.J.; Ahirwar, A.; Schoesf, B.; Bilal, M.; Saratale, G.D.; Marchand, J.; Saratale, R.G.; Varjani, S.; Vinayak, V., (2022). A techno-economic approach for eliminating dye pollutants from industrial effluent employing microalgae through microbial fuel cells: Barriers and perspectives. Environ. Res., 212: 113454 (**13 pages**).

Detjob, A.; Boonnorat, J.; Phattarapattamawong, S., (2023). Synergistic decolorization and detoxication of reactive dye navy blue 250 (NB250) and dye wastewater by the UV/Chlorine process. Environ. Eng. Res., 28(4): 220221 (**11 pages**).

Ding, Z.; Ge, Y.; Gowd, S.; Singh, E.; Kumar, V.; Chaurasia, D.; Kumar, V.; Rajendran, K.; Bhargava, P.; Wu, P.; Lin, F.; Harirchi, S.; Kumar,V.; Sirohi, R.; Sindhu, R.; Binod,P.; Taherzadeh, M.; Awasthi, M., (2023). Production of biochar from tropical fruit tree residues and ecofriendly applications–A review. Bioresour. Technol., 376: 128903 (**10 pages**).

Drenth, A.; Kema, G., (2021). The vulnerability of bananas to globally emerging disease threats. Phytopathology. 111(12): 2146-2161 (**10 pages**).

Dunne, L.; Manos, G., (2010). Perspective and introduction to adsorption and phase behaviour in nanochannels and nanotubes. In: Dunne, L.J., Manos, G. (eds) adsorption and phase behaviour in nanochannels and nanotubes. Springer, Dordrecht.

El-Nemr, M.; Ismail, I.; Abdelmonem, N.; El Nemr, A.; Ragab, S., (2021). Amination of biochar surface from watermelon peel for toxic chromium removal enhancement. Chin. J. Chem. Eng., 36:199-222 (**24 pages**).

EPA, (2024). The 12 Principles of Green Chemistry. Accessed: 18 January 2024.

Ewuzie, U.; Saliu, O.D.; Dulta, K.; Ogunniyi, S.; Bajeh, A.O.; Iwuozor, K.O.; Ighalo, J.O., (2022). A review on treatment technologies for printing and dyeing wastewater (PDW). J.

Water Process Eng., 50: 103273 (**29 pages**).

Ferreira, M.B.; de Moura Santos, E.C.M.; Nascimento, J.H.O.; Galvão, F.M.F.; dos Santos, E.V.; Santos, J.E.L.; Espinoza-Montero, P.J.; Martínez-Huitle, C.A., (2023). Electrochemical oxidation using parallel plate flow reactors as an alternative technique to treat single and trichromy dye effluents. J. Mex. Chem. Soc., 67(4): 432-447 (**16 pages**).

Fidel, R.B.; Laird, D.A.; Thompson, M.L., (2013). Evaluation of modified Boehm titration methods for use with biochars. J. Environ. Qual., 42(6): 1771-1778 (**8 pages**).

FAOSTAT, (2022). FAOSTAT statistical database. Accessed: 22 Nov 2023.

Gohil, C.; Makwana A.R., (2019). Navy blue 3G dye electrocoagulation using stainless steel electrode in presence and absence of granular activated carbon particle electrode. Int. J. Eng. Adv. Technol., 8(6): 741-745 (**5 pages**).

Guo, Y.; Yang, S.; Fu, W.; Qi, J.; Li, R.; Wang, Z.; Xu, H., (2003). Adsorption of malachite green on micro-and mesoporous rice husk-based active carbon. Dyes Pigm., 56(3), 219-229 (**11 pages**).

Guo, F.; Guo, S.; Niu, Y.; Qiu, G.; Guo, Y.; Li, Y.; Wu, J., (2023). Efficient removal of methylene blue via two-step modification hazelnut shell biochar: process intensification, kinetics and thermodynamics. J. Ind. Eng. Chem., 125:105-116 (**12 pages**).

Han, Z.; Guo, Z.; Zhang, Y.; Xiao, X.; Xu, Z.; Sun, Y., (2018). Adsorption-pyrolysis technology for recovering heavy metals in solution using contaminated biomass phytoremediation. Resour. Conserv. Recycl., 129: 20-26 (**7 pages**).

Hernández-Ortiz, M.; Durán-Muñoz, H.A.; Lozano-López, J.; Durón, S.M.; Galván-Valencia, M.; Estevez-Martínez, Y.; Ortiz-Medina, I.; Ramírez-Hernández, L.A.; Cruz-Domínguez, O.; Castaño, V.M., (2019). Determination of the surface functionality of nanocarbon allotropes by Boehm titration. Surf. Rev. Lett., 27(8): 1950190 (**7 pages**).

Hu, S.; Chang, A.; Shiue, A.; Lin, T.; Liao, S.D., (2017). Adsorption characteristics and kinetics of organic airborne contamination for the chemical filters used in the fan-filter unit (FFU) of a cleanroom. J. Taiwan Inst. Chem. Eng., 75: 87-96 (**10 pages**).

Hu, H.; Liu, J.; Xu, Z.; Zhang, L.; Cheng, B.; Ho, W., (2019). Hierarchical porous Ni/Co-LDH hollow dodecahedron with excellent adsorption property for Congo Red and Cr(VI) ions. Appl. Surf. Sci., 478: 981-990 (**10 pages**).

Hu, J.; Zhao, L.; Luo, J.; Gong, H.; Zhu, N., (2022). A sustainable reuse strategy of converting waste activated sludge into biochar for contaminants removal from water: modifications, applications and perspectives. J. Hazard. Mater., 438: 129437 (**22 pages**).

Irem, S.; Khan, Q.M.; Islam, E.; Hashmat, A.J.; ul Haq, M.A.; Afzal, M.; Mustafa, T., (2013). Enhanced removal of reactive navy blue dye using powdered orange waste. Ecol. Eng., 58: 399-405 (**7 pages**).

Jayanthi, V.; Sudarmanigayathri, N., (2015). Decolorisation of navy blue dye using a plant biomass-*Albizia amara* (silk tree). Int. J. Pharma Bio-Sci., 6(2): 584-594 (**11 pages**).

Kanchi, S.; Bisetty, K.; Kumar, G.; Sabela, M.I., (2017). Robust adsorption of direct navy blue-106 from textile industrial effluents by bio-hydrogen fermented waste derived activated carbon: equilibrium and kinetic studies. Arabian J. Chem., 10: S3084-S3096 (**13 pages**).

Kapoor, R.; Rafatullah, M.; Aljuwayid, A.; Habila, M.; Wabaidur, S.; Alam, M., (2022). Removal of patent blue dye using ananas comosus-derived biochar: equilibrium, kinetics, and phytotoxicity studies. Separations. 9(12): 426-446 (**21 pages**).

Katheresan, V.; Kansedo, J.; Lau, S., (2018). Efficiency of various recent wastewater dye removal methods: a review. J. Environ. Chem. Eng., 6(4):4676-4697 (**22 pages**).

Khaled, A.; El Nemr, A.; El-Sikaily, A.; Abdelwahab, O., (2009). Removal of direct n blue-106 from artificial textile dye effluent using activated carbon from orange peel: adsorption isotherm and kinetic studies. J. Hazard. Mater., 165: 100-110 (**11 pages**).

Khan, H.; Hussain, S.; Zahoor, R.; Arshad, M.; Umar, M.; Marwat, M.A.; Khan, A.; Khan, J.R.; Haleem, M.A., (2023). Novel modeling and optimization framework for navy blue adsorption onto eco-friendly magnetic geopolymer composite. Environ. Res., 216: 114346 (**15 pages**).

Kumar, A.; Bhattacharya, T.; Hasnain, S.; Nayak, A.; Hasnain, M., (2020). Applications of biomass-derived materials for energy production, conversion, and storage. Mater. Sci. Energy Technol., 3: 905-920 (**16 pages**).

Kumar, A.; Bhattacharya, T.; Vithanage, M., (2023). Valorization of waste biomass for biochar production and arsenic removal: a comparative assessment. Groundwater Sustainable Dev., 22: 100972 (**10 pages**).

Lapo, B.; Bou, J.J.; Hoyo, J.; Carrillo, M.; Peña, K.; Tzanov, T.; Sastre, A.M., (2020). A potential lignocellulosic biomass based on banana waste for critical rare earths recovery from aqueous solutions. Environ. Pollut., 26: 114409 (**12 pages**).

Largitte, L.; Pasquier, R., (2016). A review of the kinetics adsorption models and their application to the adsorption of lead by an activated carbon. Chem. Eng. Res. Des., 109: 495-504 (**10 pages**).

MADR, (2020). Cadena de banano. Dirección de cadenas agrícolas y forestales. Accessed: 11 Nov 2023.

Miranda-Mandujano, E.; Moeller-Chávez, G.; Villegas-Rosas, O.; Buitrón, G.; Garzón-Zúñiga, M.A., (2018). Decolourization of direct blue 2 by peroxidases obtained from an industrial soybean waste. Water SA. 44(2): 204-210 (**7 pages**).

Mishra, S.; Prabhakar, B.; Kharkar, P.; Pethe, A., (2023). Banana peel waste: an emerging cellulosic material to extract nanocrystalline cellulose. ACS Omega. 8 (1):1140-1145 (**6 pages**).

Mondal, N.; Kar, S., (2018). Potentiality of banana peel for removal of Congo red dye from aqueous solution: isotherm, kinetics and thermodynamics studies. Appl. Water Sci., 8:

1-12 (**12 pages**).
Mukherjee, S.; Thakur, A.; Goswami, R.; Mazumder, P.; Taki, K.; Vithanage, M.; Kumar, M., (2021). Efficacy of agricultural waste derived biochar for arsenic removal: tackling water quality in the Indo-Gangetic plain. J. Environ. Manage., 281: 111814 (**12 pages**).
Murphy, O.; Vashishtha, M.; Palanisamy, P.; Kumar, K., (2023). A Review on the adsorption isotherms and design calculations for the optimization of adsorbent mass and contact time. ACS Omega. 8(20): 17407-17430 (**24 pages**).
Nazir, M.; Khan, N.; Cheng, C.; Shah, S.; Najam, T.; Arshad, M.; Sharif, A.; Akhtar, S.; Rehman, A., (2020). Surface induced growth of ZIF-67 at co-layered double hydroxide: removal of methylene blue and methyl orange from water. Appl. Clay Sci., 190: 105564 (**9 pages**).
Nourmoradi, H.; Zabihollahi, S.; Pourzamani, H.R., (2016). Removal of a common textile dye, navy blue (NB), from aqueous solutions by combined process of coagulation–flocculation followed by adsorption. Desalin. Water. Treat., 55(11): 5200-5211 (**12 pages**).
Pan, X.; Gu, Z.; Chen, W.; Li, Q., (2021). Preparation of biochar and biochar composites and their application in a fenton-like process for wastewater decontamination: a review. Sci. Total Environ., 754: 142104 (**17 pages**).
Patra, B.; Mukherjee, A.; Nanda, S.; Dalai, A., (2021). Biochar production, activation and adsorptive applications: a review. Environ. Chem. Lett., 19: 2237-2259 (**23 pages**).
Pavia, D.; Lampman, G.M.; Kriz, G.S.; Vyvyan, J.A., (2014). Introduction to Spectroscopy; Cengage learning: Boston, MA, USA.
Pereira, I.C.; Carvalho, K.Q.; Passig, F.H.; Ferreira, R.C.; Rizzo-Domingues, R.C.P.; Hoppen, M.I.; Macioski, G.; Nagalli, A.; Perretto, F., (2018). Thermal and thermal-acid treated sewage sludge for the removal of dye reactive red 120: characteristics, kinetics, isotherms, thermodynamics and response surface methodology design. J. Environ. Chem. Eng., 6(6): 7233-7246 (**14 pages**).
Prabakaran, E.; Pillay, K.; Brink, H., (2022). Hydrothermal synthesis of magnetic-biochar nanocomposite derived from avocado peel and its performance as an adsorbent for the removal of methylene blue from wastewater. Mater. Today Sustainability. 18: 100123 (**14 pages**).
Prahas, D., (2008). Activated carbon from jackfruit peel waste by H_3PO_4 chemical activation: pore structure and surface chemistry characterization. Chem. Eng. J., 140: 32-42 (**11 pages**).
Priya, S.; Kennedy, J.; Anand, T., (2023). Effective conversion of waste banana bract into porous carbon electrode for supercapacitor energy storage applications. Results Surf. Interfaces. 10: 100096 (**12 pages**).
Rehman, R.; Farooq, S.; Mahmud, T., (2019). Use of agro-waste *Musa acuminata* and *Solanum tuberosum* peels for economical sorptive removal of emerald green dye in ecofriendly way. J. Cleaner Prod., 206: 819-826 (**8 pages**).
Rodríguez, A.; García, J.; Ovejero, G.; Mestanza, M., (2009). Adsorption of anionic and cationic dyes on activated carbon from aqueous solutions: equilibrium and kinetics. J. Hazard. Mater., 172: 1311-1320 (**10 pages**).
Samimi, M., (2024). Efficient biosorption of cadmium by *Eucalyptus globulus* fruit biomass using process parameters optimization. Global J. Environ. Sci. Manage., 10(1): 27-38 (**12 pages**).
Singh, S.; Parveen, N.; Gupta, H., (2018). Adsorptive decontamination of rhodamine-B from water using banana peel powder: a biosorbent. Environ. Technol. Innovation., 12: 189-195 (**7 pages**).
Sinha, P.; Datar, A.; Jeong, C.; Deng, X.; Chung, Y.; Lin, L., (2019). Surface area determination of porous materials using the Brunauer–Emmett–Teller (BET) method: limitations and improvements. J. Phys. Chem C., 123: 20195-20209 (**15 pages**).
Tkachenko, Y.; Niedzielski, P., (2022). FTIR as a method for qualitative assessment of solid samples in geochemical research: a review. Molecules. 27: 3-21 (**19 pages**).
Tovar-Gómez, R.; Moreno-Virgen, M.R.; Dena-Aguilar, J.A.; Hernández-Montoya, V.; Bonilla-Petriciolet, A.; Montes-Morán, M.A., (2013). Modeling of fixed-bed adsorption of fluoride on bone char using a hybrid neural network approach. Chem. Eng. J., 228: 1098-1109 (**12 pages**).
Wang, X.; Jiang, C.; Hou, B.; Wang, Y.; Hao, C.; Wu, J., (2018). Carbon composite lignin-based adsorbents for the adsorption of dyes. Chemosphere. 206: 587-596 (**10 pages**).
Wang, Y.; Peng, W.; Wang, J.; Chen, G.; Li, N.; Song, Y.; Chen, Z.; Yan, B.; Hou, L.; Wang, S., (2022). Sulfamethoxazole degradation by regulating active sites on distilled spirits lees-derived biochar in a continuous flow fixed bed peroxymonosulfate reactor. Appl. Catal. B: Environ., 310, 121342 (**14 pages**).
Wu, J.; Yang, J.; Feng, P.; Huang, G.; Xu, C.; Lin, B., (2020). High-efficiency removal of dyes from wastewater by fully recycling litchi peel biochar. Chemosphere. 246: 125734 (**10 pages**).
Zavvar-Mousavi, H.; Seyedi, S.R., (2010). Kinetic and equilibrium studies on the removal of Pb (II) from aqueous solution using nettle ash. J. Chil. Chem. Soc., 55(3): 307-311 (**5 pages**).
Zhao, Y.; Qamar, S.A.; Qamar, M.; Bilal, M.; Iqbal, H.M., (2021). Sustainable remediation of hazardous environmental pollutants using biochar-based nanohybrid materials. J. Environ. Manage., 300: 113762 (**24 pages**).

AUTHOR (S) BIOSKETCHES

Fuentes-Gandara, F., Ph.D., Professor, Department of Natural and Exact Sciences, Universidad de la Costa, Barranquilla, Colombia.
- Email: *fabioar20@hotmail.com*
- ORCID: 0000-0002-0681-0544
- Web of Science ResearcherID: GXV-7697-2022
- Scopus Author ID: 57192062455
- Homepage: https://www.researchgate.net/profile/Fabio-Fuentes

Piñeres-Ariza, I., Ph.D., Professor, Department of Physics, Faculty of Basic Sciences, Universidad del Atlántico, Barranquilla, Colombia.
- Email: *ismaelpineres@mail.uniatlantico.edu.co*
- ORCID: 0000-0003-4871-6211
- Web of Science ResearcherID: GQB-0840-2022
- Scopus Author ID: 56017822200
- Homepage: https://www.researchgate.net/profile/Ismael-Pineres

Zambrano-Arevalo, A., Ph.D. Candidate, Faculty of Health Sciences, Universidad Libre, Barranquilla, Colombia.
- Email: *alejandram.zambranoa@unilibre.edu.co*
- ORCID: 0000-0001-8103-7611
- Web of Science ResearcherID: GKK-9577-2022
- Scopus Author ID: 57204719770
- Homepage: https://www.researchgate.net/profile/Alejandra-Zambrano-Arevalo

Castellar-Ortega, G., Ph.D. Candidate, Faculty of Engineering, Universidad Autónoma del Caribe, Barranquilla, Colombia.
- Email: *grey.castellar@uac.edu.co*
- ORCID: 0000-0001-7711-5912
- Web of Science ResearcherID: IBJ-6846-2023
- Scopus Author ID: 57204427633
- Homepage: https://www.researchgate.net/profile/Grey-Castellar

Herrera-Herrera, C., M.Sc., Assistant Professor, Department of Natural and Exact Sciences, Universidad de la Costa, Barranquilla, Colombia.
- Email: *cherrera8@cuc.edu.co*
- ORCID: 0000-0003-1635-2003
- Web of Science ResearcherID: AAP-7558-2021
- Scopus Author ID: 57202108257
- Homepage: https://www.researchgate.net/profile/Claudia-Herrera-Herrera

Castro-Muñoz, S., B.Eng., Universidad de la Costa, Barranquilla, Colombia.
- Email: *scm950720@gmail.com*
- ORCID: 0009-0004-8364-3059
- Web of Science ResearcherID: NA
- Scopus Author ID: NA
- Homepage: https://www.researchgate.net/profile/Sharon-Catro-Munoz

Peluffo Foliaco, G., B.Eng., Universidad de la Costa, Barranquilla, Colombia.
- Email: *gabriellapeluffofoliaco@gmail.com*
- ORCID: 0009-0000-2070-8997
- Web of Science ResearcherID: NA
- Scopus Author ID: NA
- Homepage: https://www.researchgate.net/profile/Gabriela-Peluffo-Foliaco

Pinedo-Hernández, J., M.Sc., Assistant Professor, Faculty of Basic Sciences, Department of Chemistry, Universidad de Córdoba, Montería, Colombia.
- Email: *josejph@hotmail.com*
- ORCID: 0000-0002-4288-1788
- Web of Science ResearcherID: AAV-2548-2021
- Scopus Author ID: 55780076200
- Homepage: https://www.researchgate.net/profile/Jose-Pinedo-2

HOW TO CITE THIS ARTICLE

Fuentes-Gandara, F.; Piñeres-Ariza, I.; Zambrano-Arevalo, A.; Castellar-Ortega, G.; Herrera-Herrera, C., Castro-Muñoz, S.; Peluffo Foliaco, G.; Pinedo-Hernández, J., (2024). Removal of direct navy blue dye from aqueous solutions using banana peels. Global J. Environ. Sci. Manage., 10(3): 1067-1084.

DOI: 10.22034/gjesm.2024.03.09

URL: https://www.gjesm.net/article_712319.html